

On equilibrium magnetic properties in a model of repulsive particles for vortices in superconductors

Mario Nicodemi and Henrik Jeldtoft Jensen

Department of Mathematics, Imperial College, 180 Queen's Gate, London SW 7 2BZ, UK

Abstract

We study the properties of a simple lattice model of repulsive particles disordered in a pinning landscape. The behaviour of the model is very similar to the observed physics of vortices in superconductors. We compare and discuss the equilibrium phase diagram, creep dynamics, the Bean critical state profiles, hysteresis of magnetisation loops (including the second peak feature), and, in particular, "aging" in relaxations.

Important dynamical phenomena ranging from slow relaxations or hysteresis, to the anomalous "second peak" in magnetisation loops, are found in vortex physics of many different superconductors within a broad range of material parameters. This observation suggests that some basic general mechanisms are responsible for the observed phenomenology [1-4] and that schematic models from statistical mechanics can be successfully used to describe vortex matter [1,7].

We consider here a simple statistical mechanics model that appears to reproduce a very wide range of properties of vortices, ranging from dynamical behaviours to phase transitions. The model is an extension of a Multiple Occupancy cellular-automaton-like model recently introduced by Bassler and Pacuski (BP) [7] to study vortex dynamics at coarse grained level. We introduce the vortex Hamiltonian in order to be able to consider non-zero temperature effects in a consistent way and study them by Monte Carlo (MC) and replica theory methods. Our extension of the BP model also limits the occupancy of the individual lattice sites to

correctly take into account the finiteness of the upper critical field. This point is of crucial importance for the phenomenological predictions of the model. This leads us to a Restricted Occupancy Model (ROM).

We find that even the two dimensional version of the model is able to qualitatively reproduce many features similar to those observed in real superconducting samples, including a reentrant equilibrium phase diagram, creep dynamics, hysteresis of magnetisation loops, "second peak", and others. Here, in particular, we describe its equilibrium magnetic properties. The model, simple and thus tractable, nevertheless appears to capture significant aspects of the essential physics and help to establish a simple unified reference frame.

The model { A detailed description of the interaction potential, $U(r)$, between vortices depends on the considered region in the temperature-magnetic field ($T-H$) plane. For instance, at low field the London approximation can be used to derive two body potentials [2], whereas at elevated fields other approximations, such as the lowest Landau level approximation, may become relevant (see eg. [8]). Like in the BP model we consider here a coarse grained lattice version of an interacting vortex system, with a coarse graining length scale, l_0 , of the order of the natural screening length of the problem (typically, the magnetic penetration length). After coarse graining, the original interaction potential, U , is reduced to an effective Hamiltonian coupling A . In this way a drastic reduction of degrees of freedom is accomplished and the resulting schematic effective model can be more easily dealt with. The price to pay is the loss of information on scales smaller than l_0 . However, some general features of the system behaviour can survive at the level of the coarse grained description. In the above perspective, below we only consider the essential properties of vortices interaction, i.e., a mutual repulsion amongst vortices together with a spatially inhomogeneous pinning interaction. The present description can be, of course, refined by reducing the value of l_0 . We consider the Hamiltonian:

$$H = \frac{1}{2} \sum_{ij} n_i A_{ij} n_j - \frac{1}{2} \sum_i A_{ii} n_i + \sum_i A_i^p n_i \quad (1)$$

In eq.(1), $n_i \in \{0, \dots, N_{\text{eq}}\}$ is an integer occupancy variable equal to the number of particles

on site i . The parameter N_{c2} importantly bounds the particle density per site below a critical value and represents the upper critical field B_{c2} in type II superconductors. Particles also have a "charge" $s_i = \pm 1$ and neighbouring particles with opposite "charge" annihilate. The first term in eq.(1) represents the repulsion between the particles [2]. Since the coarse graining length is taken to be of order ξ we choose a finite range potential: $A_{ii} = A_0$; $A_{ij} = A_1$ if i and j are nearest neighbours; $A_{ij} = 0$ for all others couples of sites. The second term in eq.(1) just normalises the particle self-interaction energy. The third term corresponds to a random pinning potential, with a given distribution $P(A^P)$, acting on a fraction p of lattice sites (below we use $p = 1/2$). For simplicity we choose a delta-distributed random pinning: $P(A^P) = (1-p)\delta(A^P) + p\delta(A^P - A_0^P)$. To control the overall system "charge density" we can add a chemical potential term $\sum_i \mu_i S_i$ to the above Hamiltonian ($S_i = s_i n_i$). The parameters entering the model can be qualitatively related to material parameters of superconductors. The inter-vortex coupling A_0 sets the energy scale. The ratio $\kappa = A_1/A_0$ can be related to the Ginzburg-Landau parameter $\kappa = \lambda/\xi$ [9] and, in general, is expected to be an increasing function of κ . The last parameter A^P is a fraction of A_0 .

To understand the equilibrium properties of the ROM model we briefly consider its replica mean field theory (MF). In this approximation the equilibrium phase diagram in the plane $(H; T)$ (where $T = k_B T/A_1$ and $H = \Phi_0/k_B T$) can be analytically dealt with (see Fig.1). In absence of disorder it clearly shows a reentrant phase transition from a high temperature low density fluid phase to an ordered phase, in analogy to predictions in superconductors [1,5].

For moderate values of the pinning energy ($A_0^P \ll A_1$), a second order transition still takes place, which at sufficiently strong pinning is expected to become a "glassy" transition, as is seen in Random Field Ising Models [10]. For the 2D lattice we consider below (in limit $A^P \rightarrow 0$), a numerical investigation is consistent with a first order transition. In MF, the extension of the low T phase shrinks by increasing A_0^P (i.e., the highest critical temperature, T_m , decreases) and the higher is κ the smaller the reentrant region. These findings are in

agreement with experimental results on vortex phase diagrams (see Ref. [1] or, for instance, 2H-NbSe₂ superconductors from Ref. [11]).

We now go beyond MF theory and discuss the dynamical behaviour of the model. We performed MC simulations on a 2D square lattice system (we use typically $L^2 = 32^2$) described by eq.(1). The system is periodic in the y-direction and has the two opposite edges in the y-direction in contact with a reservoir of particles. The reservoir is described by H with $A_i^p = 0.8i$ and kept at a given density N_{ext} . Particles undergo diffusive dynamics and are introduced and escape the system only through the reservoir. The parameters of our simulations are usually $A_0 = 1.0$; $A_0^p = 0.3$; $N_{c2} = 27$. We have sampled several values of β [0;0.3].

We are interested in the dynamical properties of the system in the low T region of the above phase diagram. Here the 2D model has interesting magnetic hysteretic behaviours. In our MC simulations we ramp N_{ext} (starting from zero and later back to zero) at a given rate $\dot{N}_{\text{ext}} = N_0$ and record the magnetisation, $M = N_{\text{in}} - N_{\text{ext}}$ ($N_{\text{in}} = \frac{1}{L^d} \sum_{i=1}^L s_i n_i$ is the "charge" density inside the system) as a function of N_{ext} . Such a ramping induces a Bean-like profile in our lattice (inset of Fig.1) with a structure similar to some experimental data (see, for instance, [12]).

At low temperatures ($T \approx 5$ [13]), a pronounced hysteretic magnetisation loop is seen (see Fig.2), and when β is high enough ($\beta \approx 0.25$) a definite second peak appears in M . In the present case the origin of the second peak is very simple. At high density and β , groups of vortices, frustrated in minimising their repulsive interaction energy, are forced to cluster together forming macroscopically extended energetic barriers which cage other diffusing vortices. In Fig.3 we plot the average energy barrier, $\bar{E}(N_{\text{ext}})$, a particle meets during the same runs for M shown in Fig.2. A "trial" vortex approaching groups of clustered vortices has to pass over these barriers to move further. This dynamically generates the second peak. The final decrease in M at high N_{ext} is, here, due to a "softening" of these barriers caused by saturation effects related to the finite value of N_2 . The first peak in the magnetisation stems from the fact that density variations in the reservoir are only slowly transmitted in

the system when it is in the low density "fluid" phase. The second peak and hysteretic loops at moderate-high β are also present when $A_0^p \neq 0$ (A_0^p also determines the difference in the amplitude of M_j between the increasing and decreasing ramps). Very similar magnetisation data are observed in a number of different superconductors from intermediate to high values (see, for instance, refs in [4,11,14]).

The actual shape of loops strongly depends on the parameters of the dynamics (and system size). In particular, the sweep rate of the external field, \dot{h} , is very important. As soon as the inverse sweep rate is smaller than the characteristic relaxation time (which can be extremely long, inaccessible on usual observation time scales, see below) strong out-of-equilibrium effects are present, such as metastability or "memory" and "aging" [3,11,14]. As a first example of these facts, we show in the right inset of Fig.3 the dependence of the second peak height, M_p , on β . At low temperatures $T \ll 1$ and not too low ($\beta \approx 0.28$), M_p is approximately logarithmically dependent on β over several decades:

$$M_p(\beta) \sim M_0 + M \ln(\beta) \quad (2)$$

Such a behaviour gets closer to a power law $M_p \propto \beta^x$ at lower β (for instance, $x \approx 1/2$ at $\beta \approx 0.26$). Eventually, when β is smaller than a characteristic threshold, β_t , M_p exponentially saturates to its asymptotic value (this usually is orders of magnitude smaller than $M_p(\beta)$ at high β). Interestingly these findings are also very close to what is experimentally observed in superconductors [4,3]; an example from an YBCO sample (from [15]) is given in the left inset of Fig.3. The threshold, β_t , is strongly dependent on the system density N_{in} (and system size) and is a rapidly decreasing function of L ; for instance at $T = 0.3$, for $N_{ext} = N_p$ (N_p is the location of M_p), $\beta_t \approx 0.26 \times 4.5 \times 10^5$ but $\beta_t \approx 0.28 \times 10^6$. $\tau^{-1}(T; N_{in}; L)$ is a measure of the system characteristic equilibration times (which can be huge).

Seeing a dynamical phenomenon, in the ROM model the second peak is related to a true transition: in the $\beta \rightarrow 0$ limit, its location, N_p , is associated with a sharp jump in $M_{eq} \rightarrow \lim_{\beta \rightarrow 0} M(\beta)$, where its fluctuations increase with system size (see inset of Fig.2).

These findings are consistent with experiments (for instance, see Ref. [11]) and to some extents reconcile opposite descriptions ("static" v.s. "dynamic") of the phenomenon.

It is also interesting to consider the "creep rate" $Q = \frac{\partial \ln M}{\partial \ln t}$, which is often associated to a measure of the intrinsic energy barriers in the creep process [3]. Experimentally, Q is a non trivial function of the magnetic field (see for instance [15,3]). We find that, due to the very long relaxation times, $Q(N_{\text{ext}})$ is in itself a (slowly varying) function of μ , up to when μ is smaller than the smallest μ_t . In Fig.4 we show how Q depends on μ in the ROM model: for $T = 0.3$ and $\beta = 0.28$ we plot as a function of N_{ext} the average of Q over two different intervals $\mu \in [5 \cdot 10^3; 10^4]$ (filled circles) and $\mu \in [5 \cdot 10^4; 5 \cdot 10^5]$ (filled squares). The difference between the two is apparent. We note a remarkable correspondence with experimental data for YBCO, shown for the quoted sample in the inset of Fig.4.

The presence of the above "memory" effects indicate that the system, on the observed time scales, can be well off equilibrium. To reveal the underlying non-stationarity of the dynamics we consider two times correlation functions and, at a given N_{ext} , we record $\langle t > t_w \rangle$ [16]:

$$C(t; t_w) = \langle [N_{\text{in}}(t) - N_{\text{in}}(t_w)]^2 \rangle^{1/2} \quad (3)$$

Fig.5 clearly shows that $C(t; t_w)$ exhibits strong "aging": it explicitly depends on both times, contrary to situations close to equilibrium, where C is a function of the times difference $t - t_w$.

In particular at high μ and low T (where relaxation times are very high) $C(t; t_w)$ can be well

described by a generalisation of a known interpolation formula, often experimentally used [1], which now depends on the waiting time, t_w : $C(t; t_w) \sim C_1 \left[1 - \frac{h}{1 + \frac{T}{U_c} \ln \frac{t+t_0}{t_w+t_0}} \right]^{1-\alpha}$.

We found that to take $\alpha = 1$ is consistent with our data. Notice the presence of scaling properties: for not too short times C is a function of only the ratio $t-t_w$: $C(t; t_w) \sim S(t-t_w)$.

This is a fact in agreement with general scaling in off equilibrium dynamics (see Ref. [18]) and in strong analogy with other systems (from glass formers to granular media [17-20]). Experimental measurements of $C(t; t_w)$ would be very valuable.

In conclusion, in the context of a simple tractable model we depicted a panorama of

magnetic properties of vortices in type-II superconductors. Even the 2D version of the model has many interesting features in correspondence with experimental results and allows clear predictions on the nature of vortex dynamics. The origin of the slow out-of-equilibrium relaxation (observed at low T) is caused by the presence of very high free energy barriers self-generated by the strong repulsive interaction between particles at high densities (for ρ above a threshold). In this respect the pinning potential plays a minor role. For instance, the presence of a "second peak" in M , is also observed in the limit $A^p \rightarrow 0$. The second peak doesn't mark the transition to a "glassy" phase, but is also present in such a case. A^p sets the position and amplitude of the reentrant order-disorder transition line, which is in turn distinct from the second peak locations.

At low temperatures on typical observation time scales, the system is strongly out-of-equilibrium. This is most clearly seen from "aging" found in two-times correlation functions. These obey scaling properties of purely dynamical origin. Experimental check of these results would be extremely important to elucidate the true nature of vortex dynamics.

Acknowledgements We thank L. Cohen and G. Perkins for useful discussions and for the YBCO data. Work supported by the EPSRC and PRA-INFN-99.

REFERENCES

- [1] G. Blatter, M. V. Feigel'man, V. B. Geshkenbein, A. I. Larkin, V. M. Vinokur, Rev. Mod. Phys. 66, 1125 (1994).
- [2] E. H. Brandt, Rep. Prog. Phys. 58, 1465 (1995).
- [3] Y. Yeshurun, A. P. Malozemov, A. Shaulov, Rev. Mod. Phys. 68, 911 (1996).
- [4] L. F. Cohen and H. J. Jensen, Rep. Prog. Phys. 60, 1581-1672 (1997).
- [5] D. R. Nelson, Phys. Rev. Lett. 60, 1973 (1988).
- [6] M. P. A. Fisher, Phys. Rev. Lett. 62, 1415 (1989). A. Giamarchi and P. Le Doussal, Phys. Rev. Lett. 72, 1530 (1994). A. Gurevich and V. M. Vinokur, Phys. Rev. Lett. 83, 3037 (1999).
- [7] K. E. Bassler and M. Paczuski, Phys. Rev. Lett. 81, 3761 (1998). K. E. Bassler, M. Paczuski, and G. F. Reiter, Phys. Rev. Lett. 83, 3956 (1999).
- [8] A. K. Kienappell and M. A. Moore, Phys. Rev. B 60, 6795 (1999).
- [9] Asymptotically, vortex line segments interaction is exponential $V(r) = V_0 \exp(-r/\xi)$. One can write: $A_0 = A_1 / V(0) = V(\text{const.}) = 1 = \dots / \exp(\text{const.})$.
- [10] T. Nattermann, in Spin Glasses and Random Fields, ed. P. Young, (World Scientific, 1998).
- [11] K. Ghosh et al., Phys. Rev. Lett. 76, 4600 (1996); S.S. Banerjee et al., cond-mat/9911324.
- [12] D. Giller et al., Phys. Rev. Lett. 79, 2542 (1997).
- [13] We use $A_0 = 1.0$ as the energy unit and set $k_B = 1$.
- [14] Y. Paltiel et al., Nature 403, 398 (2000).

- [15] L.F. Cohen et al., *Physica C* 230, 1 (1994); G.K. Perkins et al., *Phys. Rev. B* 51, 8513 (1995). J. Totty, Ph.D. Thesis.
- [16] Time is measured in units of a MC full lattice sweep.
- [17] J.P. Bouchaud, L.F. Cugliandolo, J. Kurchan and M. Mezard, in [10].
- [18] A. Coniglio and M. Nicodemi, *Phys. Rev. E* 59, 2812 (1999).
- [19] C.A. Angell, *Science*, 267, 1924 (1995).
- [20] M. Nicodemi and A. Coniglio, *Phys. Rev. Lett.* 82, 961 (1999).

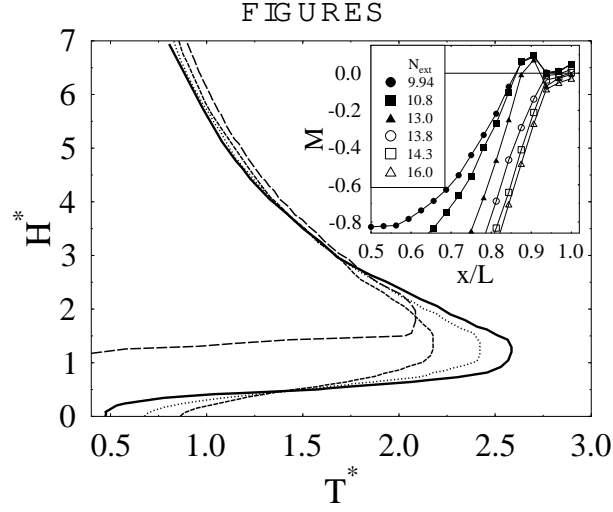


FIG. 1. Main frame The mean field phase diagram of the ROM model in the small pinning strength regime ($A_0^p < A_0$), in the plane $(H^*; T^*)$ (here $H^* = -k_B T/T = T/A_1$ are the dimensionless chemical potential and temperature), for $A_0 = 10$ and $A_0^p = 0.0; 0.5; 0.75$ (res. full, dotted and dashed lines) and $A_0 = 3.3$ and $A_0^p = 0.0$ (long dashed line). Inset The magnetisation profile, $M(x)$, as a function of the transversal spatial coordinate $x=L$ (L is the system linear size), recorded while ramping the external field, N_{ext} (for the shown values), in the 2D ROM model ($\beta = 0.26$, $T = 0.3$, $\mu = 1.1 \cdot 10^3$). Notice the change in shapes for N_{ext} smaller or larger than $N_p \approx 13.5$ (filled v.s. empty symbols).

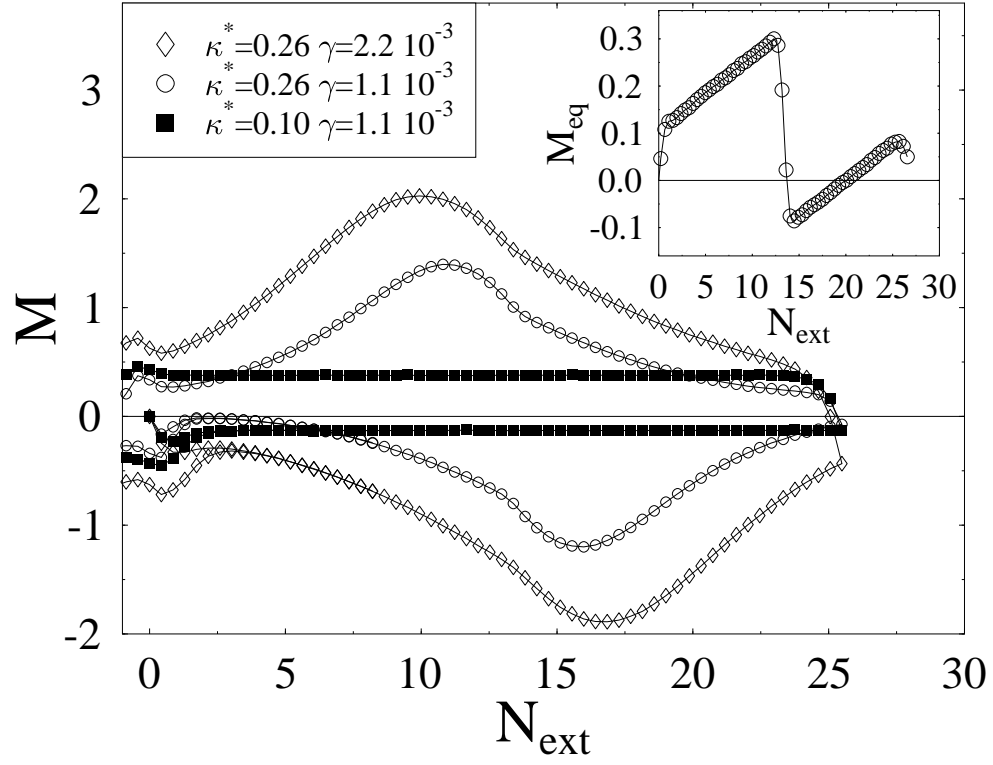


FIG. 2. Main frame The magnetisation, M , as a function of the applied field density, N_{ext} , in the 2D ROM model for $\kappa^* = 0.1; 0.26$ at $T = 0.3$ and the shown sweep rates γ . The locations of the peak, different in the increasing and decreasing branches, depend on κ^* and approach the same value in the limit $\kappa^* \rightarrow 0$. Inset The equilibrium value of M (i.e., when $\gamma \rightarrow 0$) for $\kappa^* = 0.26$ at $T = 0.3$.

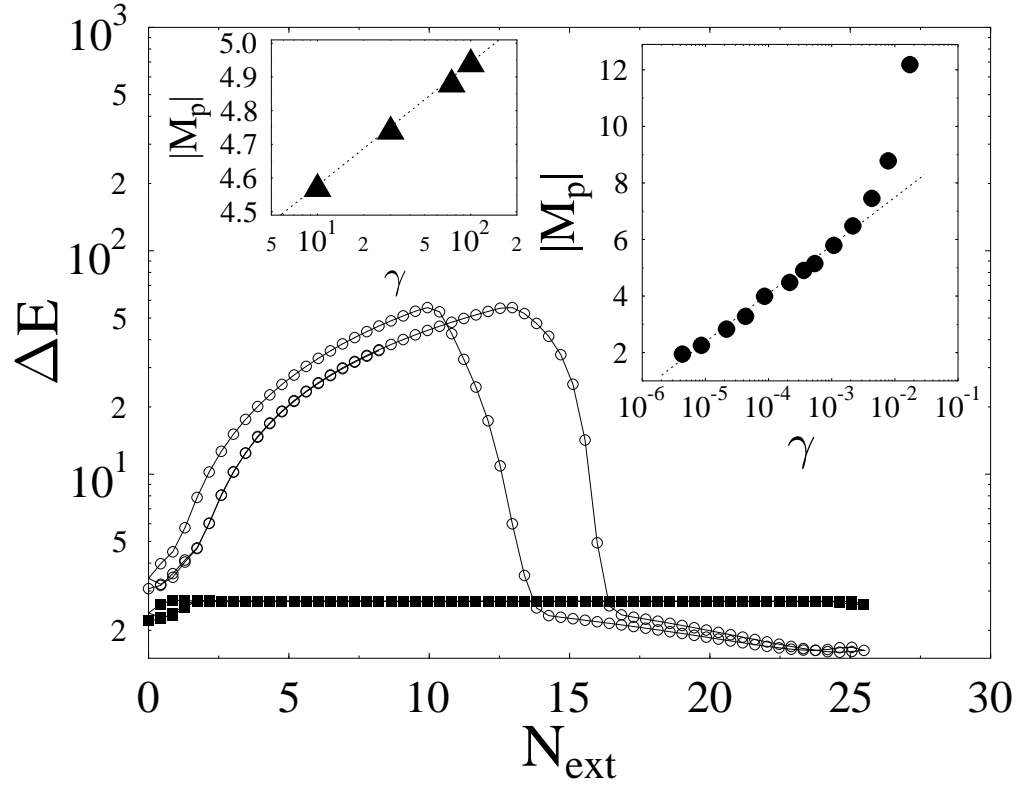


FIG. 3. Main frame The average energy barrier, E , a particle meets during diffusion in the same ROM lattices of Fig 2. Inset right The second magnetisation peak height in the ROM model as a function of the sweep rate for $A_1=A_0=0.28$ at $T=0.3$. Inset left The second magnetisation peak, M_p ($\text{Am}^2 \cdot 10^3$), in a single crystal of $\text{YBa}_2\text{Cu}_{408}$ at temperature 20K as a function of the sweep rate, \dot{H} (mT/sec) (from Ref.[15]).

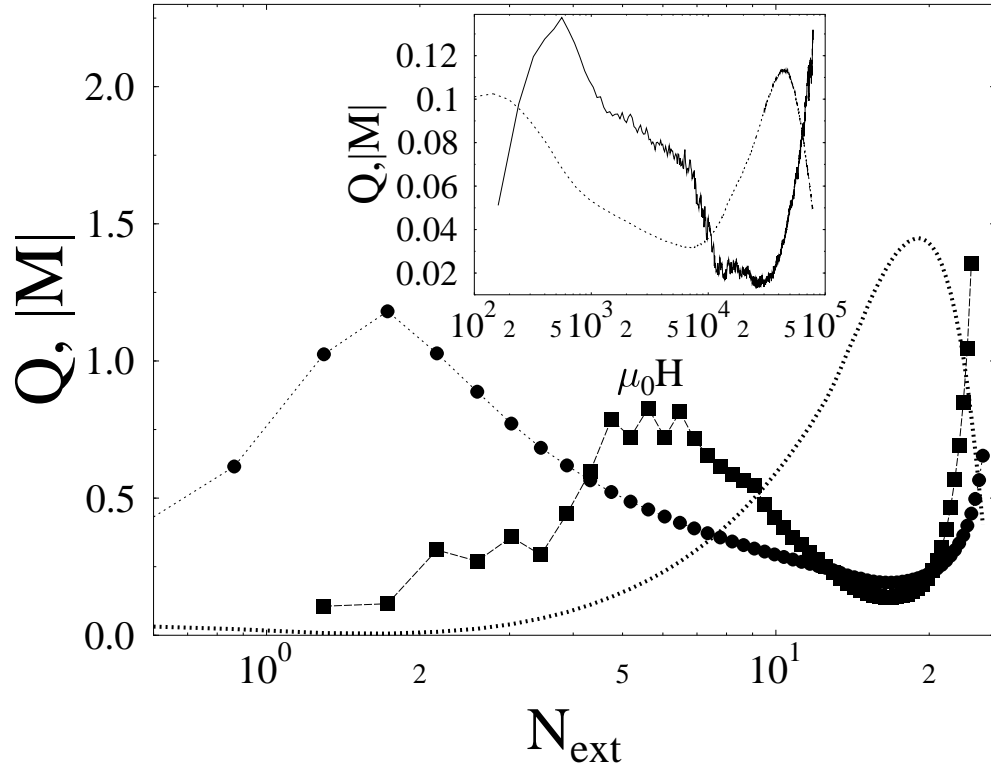


FIG. 4. Main frame For the same ROM models of the right inset of Fig.3 with $\beta = 0.28$, the "creep rate" $Q = \frac{\partial \ln M}{\partial \ln t}$ averaged over the intervals $2 \in [10^2; 10^3]$ (red circles) and $2 \in [10^4; 10^5]$ (red squares), is plotted as a function of N_{ext} . For comparison, a corresponding magnetisation loop ($M \in [-4; 4]$ to have clear scale on y-axis) is also shown (dotted line). Inset The creep rate (for $2 \in [10; 100]$ mT/sec, full line) and magnetisation loop ($4 \in [10; 100]$ mT/sec, dotted line) as a function of the external magnetic field $\mu_0 H$ (T) in the same YBaCuO sample of Fig.3.

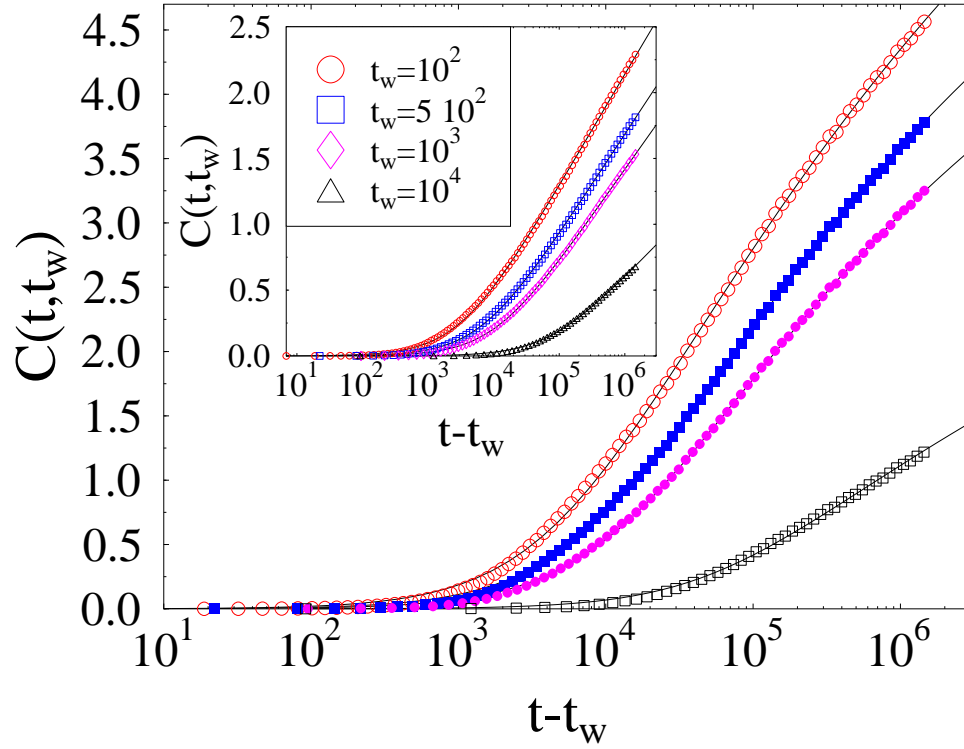


FIG. 5. Time relaxation of the two-times vortex-density correlation function, $C(t, t_w)$, in the 2D ROM model, recorded at $T = 0.1$ ($\beta = 0.28$) for the shown t_w at $N_{\text{ext}} = 4; 16$ (resp. inset, main frame). Continuous lines are logarithmic fits.